THE MECHANICS OF A THIN WEB WRAPPED HELICALLY ABOUT A TURN BAR

by

S. Müftü
Northeastern University
USA

ABSTRACT

The mechanics of the interactions between a flexible web and an externally pressurized air cushion is modeled. The web is wrapped around the porous cylindrical turn-bar at an oblique angle (helically). The turn-bar supplies pressurized air into the web/turn-bar clearance. The shell model used to represent the mechanics of the web is an extension of a previous model, and it allows the web to be wrapped around the cylinder in a helical fashion. The geometric relations are based on Rongen's work [1] and steady state equilibrium equations are developed based on the work of Müftü and Cole [2]. The fluid mechanics of the air in the web/turn-bar clearance is a two diemnsional form of the incompressible Navier-Stokes equations averaged in the clearance direction and augmented by non-linear source terms. Contact between the web and the reverser, which is undesirable in a turn-bar application, is included in the model in order to enable the analysis of the limiting cases. This paper describes the theory. Case studies and design recommendations are presented.

NOMENCLATURE

$a_{\alpha\beta}$	Metric tensor
$\vec{a}_\alpha$	Tangent vectors in curvilinear coord. (α = 1,2)
$b_{\alpha\beta}$	Curvature tensor
c	Web thickness, m
$\vec{e}_i$	Cartesian base vectors (i = 1, 2, 3)
D_b, D_t, D_s	Bend. rigidity, in-plane and shear stiffness of the web
E	Elastic modulus of the web, Pa
$E_{\alpha\beta}$	Total in-plane strain ($\alpha, \beta = x, y$)
$e_{\alpha\beta}$	Membrane strain ($\alpha, \beta = x, y$)
F_x, F_y, F_z	External tractions acting on the web, Pa
h	Web/air-reverser clearance, m
L_1, L_2	Web tangency points at $y = 0$, m
L_x, L_y	Length and width of the web, m
L^*_x, L^*_y	Length and width of the fluid domain, m
$M_{\alpha\beta}$	Bending moment ($\alpha, \beta = x, y$)
$N_{\alpha\beta}$	In-plane stress resultant ($\alpha, \beta = x, y$)
$N^{'}_{\alpha\beta}$	In-plane stress resultant ($\alpha, \beta = x, y$)
n, $\vec{n}$	Normal curvilinear coordinate and base vector
p_0	Supply pressure, Pa
p	Air pressure, Pa
p_{net}	Air pressure acting on the web, Pa
Q_α	Shear force resultant ($\alpha = x, y$)
$R(x,y)$	Web radius, m
R_c	Radius of the air-reverser, m
S	Middle surface of the web
T	Longitudinal external tension, N/m
U	Air discharge velocity at the holes, m/s
U_0	$(p_0/2\rho)^{1/2}$ reference discharge velocity, m/s
u^*, v^*	Air velocities in x^* and y^* directions, m/s
u_1, u_2	In-plane curvilinear coordinates
$w^* = w - w_r$	Web disp. with respect to reference state, m
w	Web disp. with respect to initial state, m
w_r	$w(x,L_y/2)$ reference web displacement, m
x, y	Coordinate system for the web equations
x^*, y^*	Coordinate system for the air equations
$\alpha(x^*,y^*)$	Areal hole density
β	Helical wrap angle, deg.
δ	Initial web-reverser clearance, m
γ	Shear strain
ν	Poisson's ratio of the web
κ	Discharge loss coefficient
$\kappa_{\alpha\beta}$	Web curvature ($\alpha = x, y$)
ρ	Air density, kg/m^3
θ_w	Wrap angle of the web
θ_{F1}, θ_{F2}, θ_{F3}, θ_{F4}	Limits of the hole-region in circ-dir. on the reverser, deg.
τ^*_{xy}, τ^*_{zx}, τ^*_{zy}	Fluid shear stress, Pa

INTRODUCTION

Thin, flexible, continuous structures such as paper, various forms of films, metal sheets and magnetic tapes are generally known as webs. These materials are typically processed at high transport speeds (1-20 m/s), under tension (10-200 N/m). In some of the web handling processes it is required to transport the web around a "corner" without contact. Depending on the application, air bars [3] or air reversers [2] provide an air cushion under the web to accomplish this task. In a previous article by the latter authors, a model has been introduced to analyze the case where the transport direction of the web is normal to the longitudinal axis of an air-reverser. In this paper, a more general model for the web mechanics is introduced, where the web approaches the reverser at an oblique angle, as shown in Figure 1.

The fluid structure interaction between the flexible webs and surrounding air is typically unavoidable and gives rise to interesting problems. A flexible web drags the surrounding air into the guide-web interface while it travels over rollers or stationary guides. The resulting phenomenon is known as the *foil bearing* problem and has been extensively studied, [4], [5], [6]. The foil bearing problem stems from low Reynolds number effects, hence the fluid mechanics is governed by the Reynolds lubrication equation [3].

An *air-reverser* is used in a web handling application where the transport direction of the web needs to be reversed without making contact with a rigid surface. In order to achieve this goal, the web is wrapped around a cylindrical drum with holes on its surface to provide a pressurized air layer under the web. The equations governing the mechanics of air in the web/air-reverser clearance were given in reference [7]. The web is wrapped around an air reverser in such a way that its transport (longitudinal) direction is perpendicular to the axis of the air reverser. In another type of non-contact, web support device, known as *turn-bar*, the web is wrapped around the cylinder in a helical fashion with a helix angle β. This device allows the web transport direction to be changed by an angle 2β, and thus enables more flexibility on manufacturing floor layout. In both applications the web is transported in its longitudinal direction under an externally applied tension T.

In both air-reverser and turn-bar applications pressurized air is introduced between the flexible web and the rigid cylinder from the holes on the surface of the cylinder. The clearance between the web and the cylinder is typically on the order of 3 mm. The air pressure and the web deflections are coupled. The air pressure is primarily balanced with respect to the belt-wrap pressure (T/R_c) acting on the web due to the external tension, where R_c is the radius of the air-reverser. However, creating a flow pattern under the web which will balance the belt-wrap pressure is a challenging task. The air pressure and flow pattern primarily depends on the distribution pattern of the holes on the surface of the reverser. While the flow could stagnate in the central wrap region and provide an air cushion with a fairly uniform pressure, along the four edges of the wrap region air could flow from underneath the web with speeds reaching 25 - 30 m/s. A two-dimensional air-flow model, in the plane of the web, has been introduced by Lewis [8].

In order to derive the equilibrium equations for a web in an air-reverser application, Müftü and Cole took into account the following steps the web takes until it finds equilibrium with a steady state clearance [2]. A detailed description of their model is given in their paper, and described here for completeness. The web which is initially flat is first wrapped around the cylinder, under tension T. This configuration is referred as the

Figure-2

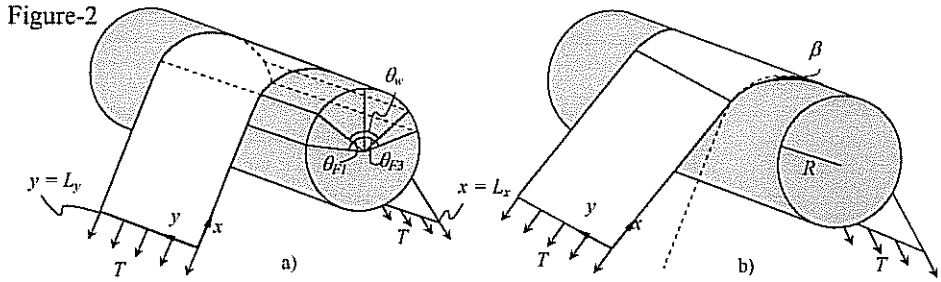

Figure 1 – Schematic representation of a) an air-reverser and b) a turn-bar

initial reference state, w_0. At this state the effect of airflow is neglected. Once the air starts coming into the interface through the holes on the reverser surface, the web deflects away from the initial reference state. During this deflection, the web tension is kept constant by a control mechanism, which allows the web length to increase between the two support-rollers on the entry and exit sides of the reverser. The web eventually finds a steady state condition which is removed from the reverser surface on the order of few millimeters. Thus the final reference state of the web from which the web deflections are measured is removed from the initial reference state and depends on the conditions such as tension and air pressure distribution of the particular application. This reference state, which is initially unknown, is called the *self-adjusting reference state*, w_r. The web deflections are measured with respect to the self-adjusting reference state. Thus the web deflection equations become non-linear. The self- adjusting reference state is a cylindrical surface extending from the mid-line of the deflected web defined as $w_r(x) = w(x,L_x/2)$. The normal component of the web deflection is measured with respect to w_r and is indicated by, $\overline{w} = w - w_r$.

In this paper the equation governing the mechanics of a flexible shell, wrapped helically around a cylinder with flat parts at the leading and trailing sides is derived. This derivation follows Rongen [1] and Müftü and Cole [2]. The equations governing the fluid flow in the web/air-reverser clearance, reported below, are essentially the same equations given by Müftü and Cole [2] with modified boundaries as described. The coupled fluid and web equations are solved numerically as described by Müftü [9].

COORDINATE SYSTEMS USED IN THE MODEL

The geometry of a web wrapped at an oblique (helix) angle β around a cylinder of radius R_c is depicted in Figure 1. Note that the web and the air-reverser can be rolled out on a plane as shown in Figure 2a. The extent of the circumferential wrap is given by the *wrap angle* θ_w as shown in this figure. The *wrap-region* spans the length $R_c\theta_w$. The projection of the *hole-region* from the air-reverser onto the web is indicated by the span $R_c(\theta_{E1} + \theta_{E2})$. The governing equations for the web displacements are expressed on the (x,y) coordinate system shown in Figure 2b. The fluid mechanics equations are expressed on a coordinate system placed on the cylindrical reverser, not shown here. The interpolation of the variables h and p between the two solution meshes is performed on the (x^*,y^*) coordinate system shown in Figure 2b.

The (x,y) coordinate system, indicated by Ω_w, for the web displacement equations is defined as;

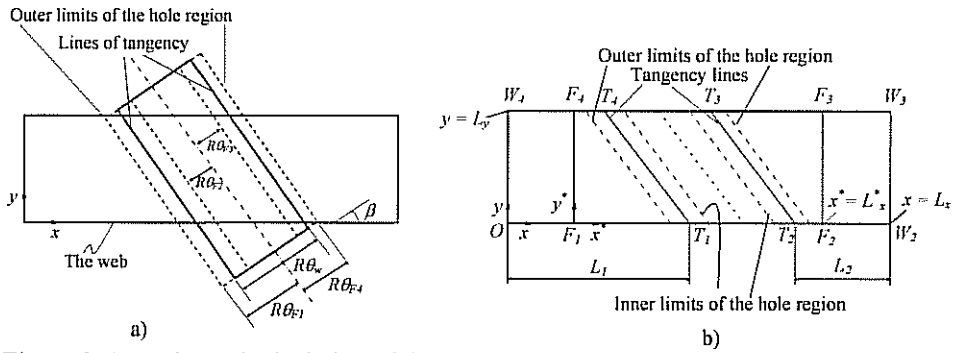

Figure-2 a) A schematic depiction of the web and the reverser rolled-out on a plane. b) The geometric definitions used to define the web Ω_w and fluid Ω_f domains.

$$\left\{(x,y)\in\Omega_w\subset R^2 \;\middle|\; 0\le x\le L_x,\;\; 0\le y\le L_y\right\}. \tag{1}$$

The coordinate system of the fluid equations (x^*,y^*) indicated by Ω_f are located on the cylindrical surface of the air-reverser. The projection of Ω_f on Ω_w is $\Omega_{f\to w}$ and it is defined as;

$$\left\{(x,y)\in\Omega_{f\to w}\subset\Omega_w \;\middle|\; y\tan\beta+x-L_{F1}\ge 0 \;\wedge\; y\tan\beta+x-L_{F2}\le 0\right\}$$

$$\text{where } L_{F1}=L_1-R\frac{\tan\left(\theta_{E1}-\frac{1}{2}\theta_w\right)}{\cos\beta} \text{ and } L_{F2}=L_2+R\frac{\tan\left(\theta_{E4}-\frac{1}{2}\theta_w\right)}{\cos\beta} \tag{2}$$

The lengths L_{F1} and L_{F2} are the projections of the outer limits of the hole-regions on the web.

EQUATIONS OF EQUILIBRIUM FOR A HELICALLY WRAPPED WEB

A web wrapped around a cylindrical surface with a helix angle β represents a developable surface. Web equilibrium equations are derived in curvilinear coordinates. The equations are written with respect to the initial reference configuration w_0, for an infinitely thin web. The geometry can be described, as shown in Figure 2b. as the union of two flat sections ($OT_1T_4W_4$ and $T_2W_2W_3T_3$) on the entry and exit sides of the wrap region, with the wrap region ($T_1T_2T_3T_4$). This figure shows the projections of the tangency points and the limits of the hole-region on the unwrapped configuration of the web, where the lines T_1T_4 and T_2T_3 are the lines of tangency. The curvilinear coordinates and the equilibrium equations with respect to this system are described by Rongen [1]. The equations of equilibrium are derived using the Kirchhoff-Love assumptions.

Geometry of a Helical Shell

The shape of a shell is usually described by its middle-surface S and thickness c. In a three dimensional space, with Cartesian basis vectors $\{\bar{e}_1,\bar{e}_2,\bar{e}_3\}$ and origin O, a generic middle-surface, is described by two independent surface coordinates u_1, and u_2 as follows,

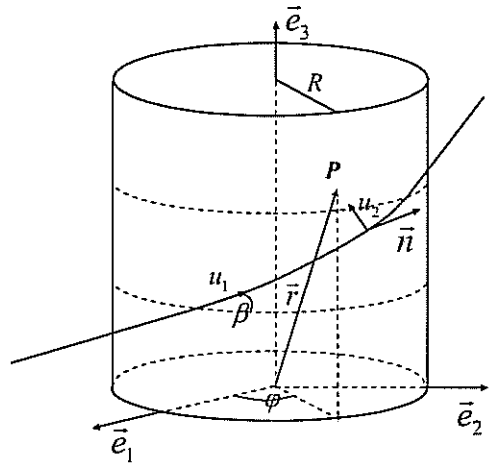

Figure-3 Coordinates of a point P on Cartesian, $\vec{e}_1, \vec{e}_2, \vec{e}_3$, and curvilinear, u_1, u_2, n coordinate systems.

$$\vec{r} = \vec{r}\left(u_1, u_2\right) = r_i\left(u_\alpha\right)\vec{e}_i \tag{3}$$

where the Latin indices take the values 1, 2, 3 and the Greek indices take the values 1 and 2. The summation convention applies to this equation where the repeated indices are summed. The location of any point $\vec{x}$ in the curved shell can then be defined by its *normal coordinates* $\left(u_1, u_2, u_3\right)$,

$$\vec{x}\left(u_1, u_2, u_3\right) = \vec{r}\left(u_1, u_2\right) + u_3\vec{n}\left(u_1, u_2\right) \tag{4}$$

where, $\vec{r}\left(u_1, u_2\right)$ is the position vector to a point on the middle surface, $\vec{n}$ is the unit normal on the middle surface at this point, and $-c/2 \le u_3 \le c/2$. The middle surface S is located at $u_3 = 0$. The *tangent vectors* to this middle-surface are defined by,

$$\vec{a}_\alpha = \vec{r}_{,\alpha} = \frac{\partial \vec{r}}{\partial u_\alpha}, \tag{5}$$

which form the base vectors for the 2-dimensional tangent plane, at each point. The *normal vector* to the middle-surface is given by,

$$\vec{n} = \frac{\vec{a}_1 \times \vec{a}_2}{\left|\vec{a}_1 \times \vec{a}_2\right|}, \tag{6}$$

providing $\vec{n}.\vec{a}_\alpha = 0$ at every point of the surface. The *first fundamental tensor* or *metric tensor* of the surface is defined by,

$$a_{\alpha\beta} = \vec{a}_\alpha.\vec{a}_\beta. \tag{7}$$

The *second fundamental tensor* or the *curvature tensor* of the surface is

$$b_{\alpha\beta} = \vec{a}_{\alpha,\beta}.\vec{n}\ . \tag{8}$$

In order to calculate the value of $\vec{a}_\alpha$ and $\vec{n}$ for the helical geometry, let us investigate the equation of the line wrapped around a cylinder with the helix angle β as shown in Figure 3. Let the curvilinear coordinates (u_1, u_2) be oriented along and perpendicular to this line, respectively. The point P on the cylindrical surface can be represented in terms of u_1, and u_2, and equation (3) as follows,

$$\begin{aligned} \vec{r} &= R\cos\varphi\vec{e}_1 + R\sin\varphi\vec{e}_2 + \left(u_1\sin\beta + u_2\cos\beta\right)\vec{e}_3, \\ &\text{with}\quad \varphi = \left(u_1\cos\beta - u_2\sin\beta\right)/R. \end{aligned} \tag{9}$$

The tangent and normal vectors for this surface are found from equations (5), (6) and (9) as follows,

$$\begin{aligned} \vec{a}_1 &= -\sin\varphi\cos\beta\vec{e}_1 + \cos\varphi\cos\beta\vec{e}_2 + \sin\beta\vec{e}_3, \\ \vec{a}_2 &= \sin\varphi\sin\beta\vec{e}_1 - \cos\varphi\sin\beta\vec{e}_2 + \cos\beta\vec{e}_3, \\ \vec{n} &= \cos\varphi\vec{e}_1 + \sin\varphi\vec{e}_2. \end{aligned} \tag{10}$$

where. The metric and the curvature tensors become,

$$a_{\alpha\beta} = \begin{bmatrix} 1 & 0 \\ 0 & 1 \end{bmatrix}, \qquad b_{\alpha\beta} = \frac{1}{R}\begin{bmatrix} -\cos^2\beta & \sin\beta\cos\beta \\ \sin\beta\cos\beta & -\sin^2\beta \end{bmatrix}. \tag{11}$$

These relations are used next to develop the equations governing the web static equilibrium equations for the helically wrapped web under tension T. The shell theory is based on the Kirchhoff-Love assumptions which state that: a) The shell is in a state of plane stress, where the normal stress in the thickness direction of the shell is neglected; and, b) A fiber of the shell which is initially straight and normal to the middle surface S, remains straight and normal to the middle surface after deformation, [10].

The in-plane displacements of the shell are indicated by v_α, and the out-of-plane displacement is by w. The strain-displacement relations for the shell then become,

$$\begin{aligned} E_{\alpha\beta} &= e_{\alpha\beta} - u_3\kappa_{\alpha\beta}, \\ E_{\alpha 3} &= \gamma_\alpha, \\ e_{\alpha\beta} &= v_{\alpha,\beta} - b_{\alpha\beta}\overline{w} + \frac{1}{2}\overline{w}_{,\alpha}\overline{w}_{,\beta}, \\ \kappa_{\alpha\beta} &= \overline{w}_{,\alpha\beta} + b_{\alpha\beta}, \\ \gamma_\alpha &= \overline{w}_{,\alpha}. \end{aligned} \tag{12}$$

where $E_{\alpha\beta}$ is the *total-strain*, $e_{\alpha\beta}$ is the *membrane-strain*, γ_α is the *shear-strain*, $\kappa_{\alpha\beta}$ is the *curvature* of the middle surface. Note that the curvature $b_{\alpha\beta}$ is added to the curvature of the middle-surface in order to take into account the initial bending of the web around the cylindrical surface.

The in-plane stresses in the deformed shell are indicated by $\sigma_{\alpha\beta}$ and the shear stresses in the direction normal to the middle surface S are indicated by $\sigma_{\alpha 3}$. The shell theory is based on stress resultants which are defined as follows,

$$\left(N_{\alpha\beta}, M_{\alpha\beta}, Q_\alpha\right) = \int_{-c/2}^{c/2} \left(\sigma_{\alpha\beta}, u_3\sigma_{\alpha\beta}, \sigma_{\alpha 3}\right) du_3 \tag{13}$$

where $N_{\alpha\beta}$ are the in-plane stress resultants, $M_{\alpha\beta}$ are the bending moment resultants and Q_α are the normal shear stress resultants. The static equilibrium of a curved shell is given by the following set of equations,

$$\begin{aligned} N_{\alpha\beta,\beta} + F_\alpha &= 0 \\ Q_{\alpha,\beta} + \left(w_{,\alpha} N_{\alpha\beta}\right) + b_{\alpha\beta} N_{\alpha\beta} + F_z &= 0 \\ M_{\alpha\beta,\beta} - Q_\alpha + C_\alpha &= 0 \end{aligned} \tag{14}$$

where F_α, C_α and F_z are the external in-plane force, bending moment and pressure, respectively. Equations (14a,b) represent the static equilibrium of in-plane and out-of-plane forces, respectively. Equation (14c) is the moment equilibrium equation.

For an isotropic shell the constitutive equations are,

$$\begin{aligned} N_{\alpha\beta} &= D_t\left[\left(1-\upsilon\right)e_{\alpha\beta} + \upsilon a_{\alpha\beta} e_{\pi\pi}\right] \\ M_{\alpha\beta} &= -D_b\left[\left(1-\upsilon\right)\kappa_{\alpha\beta} + \upsilon a_{\alpha\beta}\kappa_{\pi\pi}\right] \\ Q_\alpha &= D_s\gamma_\alpha \end{aligned} \tag{15}$$

where $D_b = Ec^3/12\left(1-\upsilon^2\right)$ is the bending rigidity, $D_t = Ec/\left(1-\upsilon^2\right)$ is the in-plane stiffness and $D_s = \kappa Gc$ is the shear stiffness, with the Young's modulus E, shear modulus G and shear correction coefficient κ. The correction coefficient usually takes the value of 5/6.

The mechanics of the web is described with respect to a set of curvilinear coordinates located on the web (x, y, n). Note that these coordinates are identical to (u_1, u_2, n) coordinates indicated in the previous figures. After combining equations (14b) and (14c) the equilibrium equations become,

$$N_{\alpha\beta,\beta} + F_\alpha = 0,$$
$$M_{\alpha\beta,\alpha\beta} + \left(w_{,\alpha} N_{\alpha\beta}\right)_{,\beta} + b_{\alpha\beta} N_{\alpha\beta} + F_z = 0. \tag{16}$$

By using moment curvature relations, (15b), and the curvature tensor, (11), equation (16) becomes,

$$N_{xx,x} + N_{xy,y} + F_x = 0,$$
$$N_{yx,x} + N_{yy,y} + F_y = 0,$$
$$D_b \nabla^4 \overline{w} - \left(w_{,xx} - \frac{\cos^2\beta}{R_w}\right) N_{xx} - 2\left(w_{,xy} - \frac{\sin\beta\cos\beta}{R_w}\right) N_{xy} - \left(w_{,yy} - \frac{\sin^2\beta}{R_w}\right) N_{yy} = F_z. \tag{17}$$

where $R_w = R_w(x,y)$ is the radius of curvature of the shell defined as,

$$\frac{1}{R_w(x,y)} = \begin{cases} 0, & \text{for } x + y\tan\beta - L_1 < 0 \\ \dfrac{1}{R_c}, & \text{for } x + y\tan\beta - L_1 \geq 0 \text{ and } x+y\tan\beta - L_2 \leq 0 \\ 0, & \text{for } x + y\tan\beta - L_2 > 0 \end{cases}. \tag{18}$$

where L_1 and L_2 are the tangency points at $y = 0$. Equation (17) represents a set of coupled partial differential equations, which in turn represent the equilibrium of a shell wrapped around a cylinder in a helical fashion, with a helix angle β, as described in Figure 1, subjected to in-plane forces F_x and F_y and external pressure p.

In a typical web handling application, the web is pre-tensioned to a value T in the longitudinal direction. It is assumed that, in the undeformed state, only T exists as in-plane stress, when the web is wrapped around the cylinder. The in-plane stress resultants after deformation are indicated as follows,

$$N_{xx} = T + N'_{xx}, \quad N_{yy} = N'_{yy}, \quad N_{xy} = N'_{xy}, \tag{19}$$

A simplified equation which represents the equilibrium of out-of-plane force resultants and bending moments can be obtained by considering that N'_{xx} can be evaluated in terms of deformations by using the strain-displacement relations, (12), and the constitutive relation, (15). Thus the in-plane stress resultant in the longitudinal direction becomes,

$$N_{xx} = T + D_t\left[\frac{\overline{w}}{R_w}\cos^2\beta + \frac{1}{2}\overline{w}_{,x}^2 + \nu\left(\frac{\overline{w}}{R_w}\sin^2\beta + \frac{1}{2}\overline{w}_{,y}^2\right)\right] \tag{20}$$

Then using the above equations it can be shown that the equation of equilibrium for a flexible web wrapped around a cylindrical drum with a helix angle β is,

$$D_b \nabla^4 \overline{w} + D_t \left(\cos^4 \beta + \nu \cos^2 \beta \sin^2 \beta \right) \frac{\overline{w}}{R_w^2(x,y)} - T w_{,xx} = p + p_c - \frac{T \cos^2 \beta}{R_w} \qquad (21)$$

Note that for $\beta = 0$ this equation reduces to the same web equilibrium equation derived for the case of no helix angle [2]. Note that the vertical component of the external traction F_z in Equation (17), has been replaced with the air pressure p and the contact pressure p_c. The air and contact pressure distributions are obtained from the solution of the fluid mechanics equations, and evaluation of the contact conditions as presented in the next sections.

The web is supported by a roller on each of its two longitudinal ends, and is free on its lateral edges. These conditions are represented as simple support conditions,

$$\begin{aligned} \overline{w} &= 0, \\ M_x &= D_b \left[\overline{w}_{,xx} + \upsilon \overline{w}_{,yy} \right] = 0, \end{aligned} \qquad (22)$$

at $0 \le y \le L_y$ and $x = 0, L_x$, and as free boundary conditions,

$$\begin{aligned} M_y &= D_b \left[\overline{w}_{,yy} + \upsilon \overline{w}_{,xx} \right] = 0, \\ Q_y &= D_b \left[\overline{w}_{,yyy} + (2 - \upsilon) \overline{w}_{,xxy} \right] = 0, \end{aligned} \qquad (23)$$

at $y = 0, L_y$ and $0 \le x \le L_x$.

Initial Clearance. The clearance $h(x,y)$ between the web and the turn-bar depends on the initial clearance $\delta(x,y)$ and the web displacement w,

$$h(x,y) = w(x,y) + \delta(x,y) \qquad (24)$$

The initial clearance in the downstream and upstream sides of the web is obtained by calculating the distance between the web and the cylinder. In the wrap region, the initial clearance is zero. This is expressed by the following relation,

$$\delta(x,y) = \begin{cases} \left((x + y \tan\beta - L_1)^2 \cos^2 \beta + R^2 \right)^{1/2} - R, & \{(x,y) \in \Omega_w \,|\, y \tan\beta + x - L_1 < 0\} \\ 0, & \{(x,y) \in \Omega_w \,|\, y \tan\beta + x - L_1 \ge 0 \ \wedge \ y \tan\beta + x - L_2 \le 0\} \\ \left((x + y \tan\beta - L_2)^2 \cos^2 \beta + R^2 \right)^{1/2} - R, & \{(x,y) \in \Omega_w \,|\, y \tan\beta + x - L_2 > 0\} \end{cases} \qquad (25)$$

In obtaining the equations for the curvature and the initial clearance, the effect of bending rigidity of the web is neglected; and, the web is assumed to consist of two flat segments and one "helically-wrapped cylindrical" segment.

EQUATIONS OF FLUID MECHANICS

The steady state form of the equations governing the fluid mechanics in the clearance between the web and the turn bar were derived by Lewis [7]. As the clearance $h(x^*,y^*)$ between the web and the reverser is considerably smaller as compared to the other two dimensions of the fluid domain, namely x^* and y^* directions, the flow is assumed two dimensional in the plane of the reverser. Thus the flow velocities u^* and v^* in the x^* and y^* directions, respectively, are averaged in the direction of the clearance height, and the flow component in the z^* direction is neglected. The effect of the air coming into the interface through the holes is modeled as a distributed source, indicated by $\alpha(x^*,y^*)$. Velocity of air U coming through each hole is a function of the supply pressure inside the reverser p_0 and the local pressure of air p. The two-dimensional flow assumption is invalid near each hole, and losses due to discharge are represented with the discharge coefficient κ, whose value lies in the range (0,1]. The air velocity through each hole is modeled as follows,

In their final form these equations contain distributed source terms to model the effects of the air injected through the holes. These equations also include the effects of air viscosity and turbulence. They are given as follows,

$$U = \kappa U_0 \left(1 - \frac{p}{p_0}\right)^{1/2} \tag{26}$$

where the reference discharge velocity $U_0 = \left(p_0/2\rho\right)^{1/2}$. The conservation of mass is given by,

$$\frac{\partial hu^*}{\partial x^*} + \frac{\partial hv^*}{\partial y^*} = \alpha U\,, \tag{27}$$

where the term on the right hand side represents the mass of air coming into the interface through the air holes. The conservation of momentum in the x^* and y^* directions is represented by the following two equations,

$$\begin{aligned}
&\rho\left(u^*\frac{\partial u^*}{\partial x^*} + v^*\frac{\partial u^*}{\partial y^*}\right) + \frac{\partial p}{\partial x^*} - \mu\left(\frac{4}{3}\frac{\partial^2 u^*}{\partial x^{*2}} + \frac{\partial^2 u^*}{\partial y^{*2}} + \frac{1}{3}\frac{\partial^2 v^*}{\partial x^*\partial y^*}\right) + 2\frac{\tau^*_{z^*x^*}}{h} + \alpha\rho U\frac{u^*}{h} = 0 \\
&\rho\left(u^*\frac{\partial v^*}{\partial x^*} + v^*\frac{\partial v^*}{\partial y^*}\right) + \frac{\partial p}{\partial y^*} - \mu\left(\frac{\partial^2 v^*}{\partial x^{*2}} + \frac{4}{3}\frac{\partial^2 v^*}{\partial y^{*2}} + \frac{1}{3}\frac{\partial^2 u^*}{\partial x^*\partial y^*}\right) + 2\frac{\tau^*_{z^*y^*}}{h} + \alpha\rho U\frac{v^*}{h} = 0
\end{aligned} \tag{28}$$

where, ρ is the mass density, μ is the viscosity of air, and p is the air pressure averaged over the normal direction. The flow is turbulent in the web-reverser clearance, as indicated by the high value of the Reynolds number, (Re=O(5000)) [2]. The shear stresses $\tau_{z^*x^*}$ and $\tau_{z^*y^*}$ are found from the 1/7th-power-velocity distribution law for turbulent flow in a two-dimensional channel [11],

Case	$\theta_{F1} - \theta_{F2}$	$\theta_{F3} - \theta_{F4}$
1	$-90^{\circ} - -50^{\circ}$	$50^{\circ} - 90^{\circ}$
2	$-100^{\circ} - -60^{\circ}$	$60^{\circ} - 100^{\circ}$
3	$-110^{\circ} - -70^{\circ}$	$70^{\circ} - 110^{\circ}$

Table 1. The extent of the hole-regions for the three cases discussed in this paper. See Figure 1 and 2a for the definitions of the angles θ_{Fi}.

$$\tau_{z^*x^*} = \frac{1}{2}\rho 0.0676 \cos\bar{\theta}\left(\frac{\rho h}{\mu}\right)^{\lambda'}\left(u^{*2}+v^{*2}\right)^{\left(2-\lambda'\right)/2}$$
$$\tau_{z^*y^*} = \frac{1}{2}\rho 0.0676 \cos\bar{\theta}\left(\frac{\rho h}{\mu}\right)^{\lambda'}\left(u^{*2}+v^{*2}\right)^{\left(2-\lambda'\right)/2} \tag{29}$$

with $\bar{\theta} = \tan^{-1}\left(u^{*}/v^{*}\right)$ and $\lambda' = 1/4$. The solution of this equation is discussed in [8].

The boundary Γ_f of the fluid solution domain is the outer periphery of the parallelogram defined as,

$$\left\{\Gamma_f \middle| \left(x^*, y^*\right) \in \Omega_f \subset R^2,\ \left(x^*, 0\right) \wedge \left(x^*, L_y^*\right) \wedge y^* \tan\beta + x^* - L_{x1}^* = 0 \wedge y^* \tan\beta + x^* - L_{x2}^* = 0\right\} \tag{30}$$

where L_{F1}^* and L_{F2}^* are the limits of the hole regions at $y^* = 0$. Given these, the boundary condition for fluid becomes,

$$p + \frac{1}{2}\kappa_B\left(\left(u^*\right)^2 + \left(v^*\right)^2\right) = 0 \quad \text{on } \Gamma_f \tag{31}$$

where κ_B is the boundary discharge coefficient.

CONTACT PRESSURE

In case rigid body contact occurs between the web and the reverser surface, the web is supported (partially) by the contact pressure p_c. Whether contact will take place depends on the overall equilibrium of the web and the air pressure. If contact occurs, its magnitude, and location are not known apriori. In general, surfaces are not smooth; and, contact between two surfaces takes place on the peaks of the surface asperities. A review of available multi-asperity contact models is beyond the scope of this paper. However, in the context of web and tape mechanics papers by Rice et al. [12], Lacey and Talke [13], and Wu and Talke [14] could be consulted for more information. In this work, the parabolic contact model introduced by Lacey and Talke for tape mechanics is used. This

model was later evaluated by Rice et. al for contact of paper and PET based webs. In this model the contact pressure is evaluated by,

$$p_c = P_0\left(1-\frac{h}{\sigma_0}\right)^2 \quad \text{if } h \le \sigma_0 \tag{32}$$

where P_0 is the asperity compliance and σ_0 is the asperity engagement height. If the web-to-reverser clearance h falls below σ_0 then it is assumed that asperity contact takes place. The values of P_0 and σ_0 are typically empirically determined. For web contact guidance on these selections are given in reference [12]. In this paper the following values were used.: $P_0 = 1\times10^6$ Pa and $\sigma_0 = 100\times10^{-6}$ m.

RESULTS AND DISCUSSION

In order to investigate the effect of helical wrap, a case study of different helix angles varying in the range of $0^\circ \le \beta \le 45^\circ$, is conducted. In this study the web wrap angle around the reverser, is $\theta_w = 180^\circ$. Three different cases of hole distributions were investigated. In all three of these cases, the total span of the main hole-regions are 40° in the entry and 40° exit directions of the web. This 40° window is moved around in the circumferential direction, in order to investigate the effect of placing the hole-region in relation to the wrap region. The three cases of hole region locations are defined in Table 1. All of the other parameters were kept constant at their values reported in Tables 2 and 3. The node spacing used for the finite difference solution are reported in Table 3.

The steady state conditions for $\beta = 0^\circ$ and 45°, for case-1, are plotted in Figures 4 and 5, respectively. The web displacement (w) distribution, measured with respect to the initial wrapped state, is plotted in part a) of these figures. The air velocity distribution in the fluid domain is given in part b), where the air pressure (p) contours are also plotted. Finally, the air pressure and contact pressure (p_c) profiles are plotted in 3D in parts c) and d). Note that the same legends are used in these figures.

E (GPa)	4	μ (Pa.s)	1.85×10^{-5}
ν	0.3	R (m)	0.1
c (mm)	0.05	θ_w (deg.)	180
T_x (N/m)	40	κ	0.9
ρ (kg/m^3)	1	p_o (kPa)	0.8, 1, 1.2, 1.4

Table 2. Parameters common to the presented cases.

β	0°	5°	10°	15°	20°	30°	40°	45°
L_1 (m)	1	1	1	1	1	1	1	1
L_2 (m)	0.96	0.91	0.87	0.82	0.71	0.58	0.71	0.50
L_x (m)	2.31	2.27	2.23	2.19	2.15	2.07	1.99	1.95
L_y (m)	0.50	0.50	0.50	0.51	0.51	0.51	0.51	0.50
Δx=Δy (mm)	5.78	5.68	5.58	5.48	5.38	5.18	4.96	4.87
Δx^* (cm)	0.88	0.90	1.11	1.25	1.39	1.75	2.21	2.48
Δy^* (cm)	1.24	1.25	1.26	1.26	1.26	1.27	1.27	1.24

Table 3. Length parameters used for the presented cases.

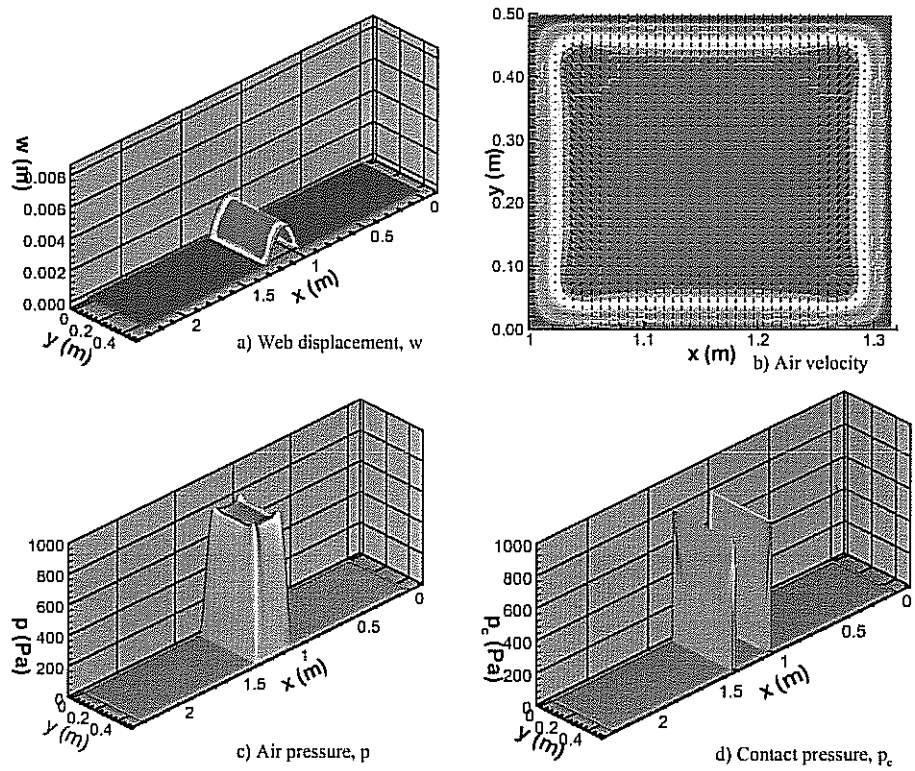

Figure-4 The steady state conditions for the case-1, with $\beta = 0^{\circ}$, $p_0 = 800$ Pa

In general, Figure 4a and 5a show a large displacement in the wrap region, where the web is supported by the air cushion. In the case of $\beta = 0^{\circ}$, the maximum displacement is on the order of 2 mm. But, when the web is wrapped with a helix angle of $\beta = 45^{\circ}$ the maximum web displacement is found to be approximately 8 mm. In both of these figures, the air cushion support is insufficient to prevent web contact at the entry end exit regions. This is evidenced by the non-zero contact pressure distribution shown in Figures 4d and 5d. Noted that the non-smooth contact pressur shown in Figure 5d is the result of numerical discretization. Nevertheless, the web is supported in the central wrap region by the air cushion. In the case of zero wrap-angle, Figure 4c shows that, in the central region, the air pressure settles to approximately 800 Pa; the pressure drops to ambient in a narrow transitional region around the outer periphery of the wrap region. On the other hand, the air pressure for the wrap-angle of $\beta = 45^{\circ}$ settles to approximately 450 Pa in the central wrap-region. The pressure drops to ambient in a similar manner around the outer periphery.

The magnitudes of the pressure contours and web displacements at steady state are strongly influenced by the helix angle. At the low value of β (Figure 4), the steady state pressure contours reach 800 Pa range, whereas at the high value of β (Figure 5), the contours reach 450 Pa range. Conversely, the web displacement is lower for low values of β, whereas it is higher for higher values. In fact, as the helix angle increases from 0° to 45° the web displacement increases while the maximum pressure decreases. This may at

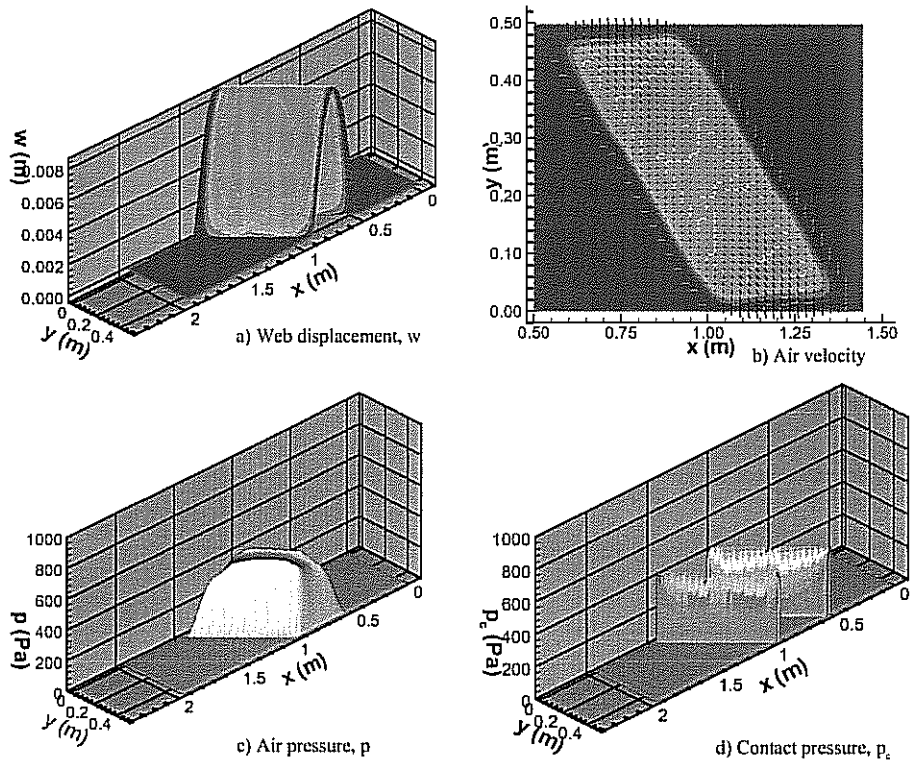

Figure-5 The steady state conditions for the case-1, with $\beta = 45^{\circ}$, $p_0 = 800$ Pa.

first seem counter intuitive; However, it is actually due to the β dependence of the shell-stiffness and the belt-wrap pressure. Equation (21) shows that the *shell-stiffness* and the *belt-wrap pressure* for the helically-wrapped web are defined as,

$$D_t\left(\cos^4\beta + \nu\cos^2\beta\sin^2\beta\right) \quad \text{and} \quad \frac{T\cos^2\beta}{R_w},$$

respectively. Thus it can easily be seen that the effect of both of these parameters reduce at when $\beta > 0$. As the belt-wrap pressure is reduced at higher β values, the overall equilibrium is established at lower air pressure levels. Similarly, the shell stiffness is also reduced as a result of increasing β, resulting in a more compliant web behavior.

Effect of the supply pressure on the three cases of hole distributions is presented in Figures 6 - 8 for p_0 values of 800, 1000, 1200 and 1400 Pa. For Case-1, where the hole-region is placed right on the boundary of the web's tangency line, the air pressure is insufficient to overcome the belt-wrap pressure and the web contacts the reverser surface near the tangency lines. Increasing supply pressure only ends up lifting the web in the central region, otherwise the web remains in contact on the tangency line, as shown in Figure 6.

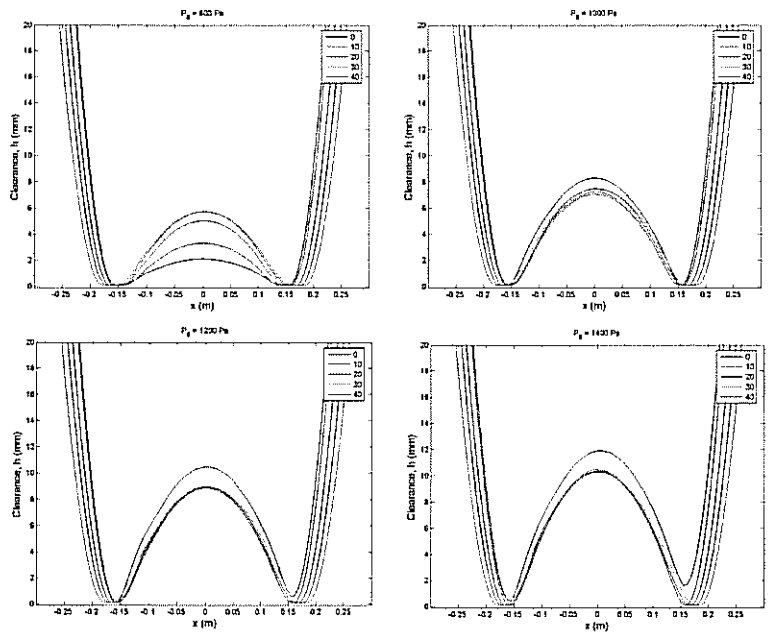

Figure - 6 Center line (x,L_y/2) displacements for the Case-1, for supply pressure values of p_0 = 800, 1000, 1200, 1400 Pa, in figures a) – c), respectively, and helix angles of β = 0, 10, 20, 30, 40 deg.

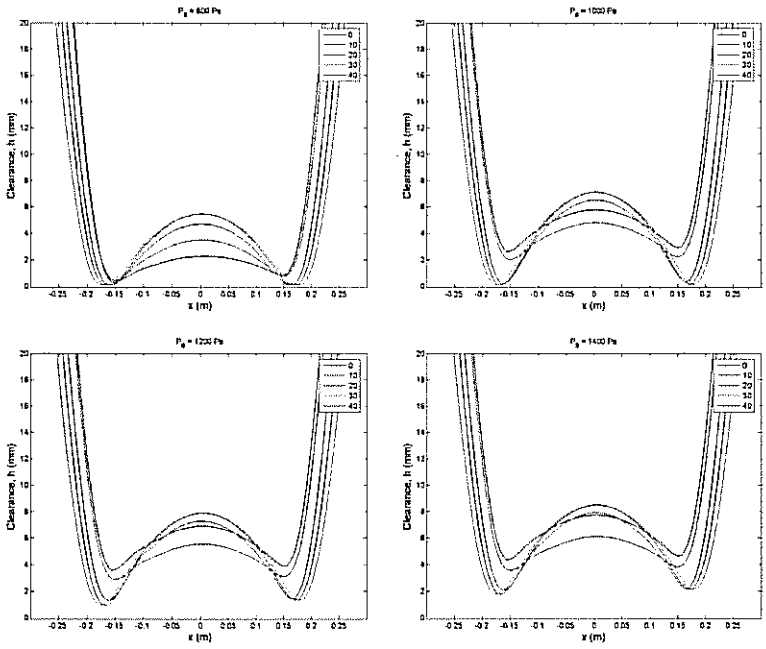

Figure - 7 Center line (x,L_y/2) displacements for the Case-2, for supply pressure values of p_0 = 800, 1000, 1200, 1400 Pa, in figures a) – c), respectively, and helix angles of β = 0, 10, 20, 30, 40 deg.

In Case-2, where the hole-region encloses the web's tangency lines, the web contacts the reverser only for the lowest supply pressure value of p_0 = 800, for the helix angles of

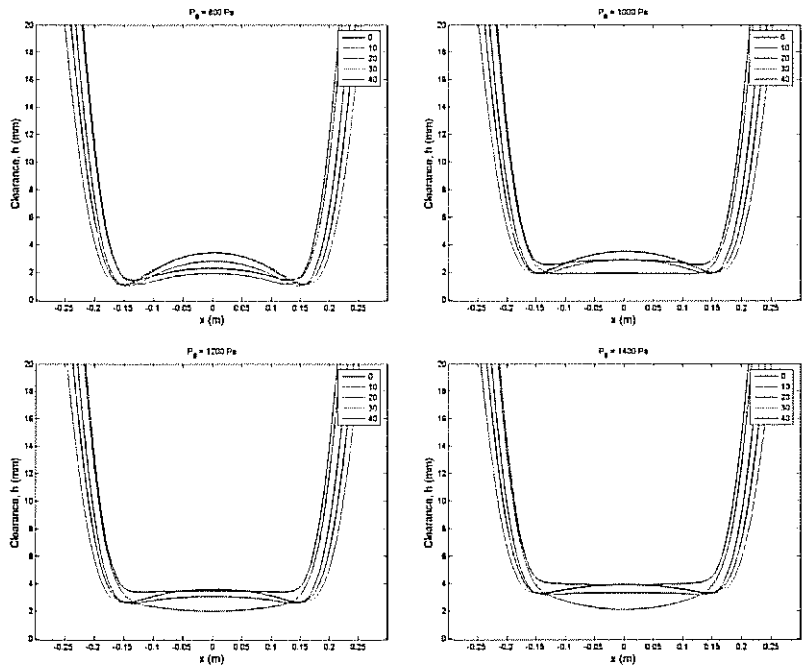

Figure - 8 Center line (x,L_y/2) displacements for the Case-3, for supply pressure values of p_0 = 800, 1000, 1200, 1400 Pa, in figures a) – c), respectively, and helix angles of β = 0, 10, 20, 30, 40 deg.

20°, 30° and 40°, as shown in Figure 7. For all of the other supply pressures and helical wrap angles no contact occurs. In general increasing supply pressure and increasing helix angle causes the web displacement to increase. For this hole-distribution the web displacement near the tangency line is significantly lower as compared to the central region of the web.

In Case-3, where the hole-region spans the 110° to 70° range, on the entry and exit of the air reverser, the web displacement in the wrap region is more uniform, as can be observed in Figure 8. However, the overall, web displacements are lower than those in Case-2. Considering that no contact occurs for any of the supply pressure values and helix angles, this is a safer design for preventing web contacts.

SUMMARY

A mathematical model for the steady state deformations of a web wrapped around an air-reverser in a helical fashion is developed. This is an extension of a previous model where the helix angle was zero [2]. An equation governing the steady state deformations of a thin flexible, cylindrical shell is derived. These equations show that the shell stiffness and the belt-wrap pressure are both reduced due to the helical wrap. The equations governing the fluid mechanics of the air cushion between the web and the air-reverser is modified to accommodate skewed boundaries. The coupled system is solved numerically. A case study shows that increasing helix-angle results in increased web-reverser separation and lower steady state air pressure. This study also shows that, in order to

prevent web-scratches, it is advantageous to place the hole-regions circumferentially, on the reverser, in such a way that they to enclose the tangency points of the web.

REFERENCES

[1] Rongen, P. M. J., "Finite Element Analysis of the Tape Scanner Interface in Helical Scan Recording" Ph.D. Dissertation, Technische Univesiteit Eindhoven, The Netherlands, 1994.

[2] Müftü, S., Cole, K.A., "The fluid/structure interaction of a thin flexible cylindrical web supported by an air cushion," Journal of Fluids and Structures, Vol. 13, 1999, pp. 681-708.

[3] Gross, W. A., 1980. Fluid Film Lubrication. John Wiley and Sons, New York.

[4] Ducotey, K.S., Good, J.K., "Predicting traction in web handling," ASME Journal of Tribology, Vol. 121, 1999, pp. 618-624.

[5] Müftü, S., Altan, M.C., "Mechanics of a porous web moving over a rigid guide," ASME Journal of Tribology, Vol. 122, 2000, pp. 418-426.

[6] Hashimoto, H., Nakagawa, H., "Improvement of web spacing and friction characteristics by two types of stationary guides," ASME Journal of Tribology, Vol. 123, 2001, pp. 509-518.

[7] Müftü, S., Lewis, T.S., Cole, K.A., Benson, R.C., "A two dimensional model of the fluid dynamics of an air reverser," ASME Journal of Applied Mechanics, Vol. 65, 1998, pp. 171-177.

[8] Müftü, S., Lewis, T.S., Cole, K.A., "A numerical solution of the Euler's equations with nonlinear source terms in modeling the fluid dynamics of an air reverser," Proceedings of the I.S.P.S., ASME International Congress and Exposition, Dallas, TX, November 1997, pp. 39-48.

[9] Müftü, S., "Numerical solution of the equations governing the steady state of a thin cylindrical web supported by an air cushion," Proceedings of the ASME Noise Control and Acoustics Division-1999 **NCA-26**, 1999, pp. 425-434.

[10] Timoshenko, S.P., Woinkowsky-Krieger, S., 1987. Theory of Plates and Shells. McGraw-Hill, New York, 1987.

[11] Schilcting, H., Boundary-Layer Theory. New York: McGraw-Hill, 1987.

[12] Rice, B., Cole, K.A. and Müftü, S., "A model for determining the asperity engagement height in relation to web traction over non-vented rollers," ASME Journal of Tribology, *Vol.* 124, No.3, 2002, pp. 584-594.

[13] Lacey, C. and Talke, F., "Measurement and simulation of partial contact at the head/tape interface," ASME Journal of Tribology, Vol. 144, 1992, pp. 646-652.

[14] Wu, Y., Talke, F., "The Effect of Surface Roughness on the Head-tape Interface," ASME Journal of Tribology, Vol. 118, No. 2, 1996, pp. 376-381.

Name & Affiliation	
	Question Have you ever conducted this kind of research on a porous web?
Name & Affiliation Sinan Müftü Northeastern University	**Answer** No, we haven't.
Name & Affiliation	**Question** Do you have any plans in the future?
Name & Affiliation Sinan Müftü Northeastern University	**Answer** Yes, if someone supports it definitely.
Name & Affiliation Steve Lang Proctor & Gamble	**Question** I was interested in your finding that the shell stiffness was reduced. Would you expect that to affect wrinkle tendencies for this? Would you adjust say the radius or tension to accommodate that?
Name & Affiliation Sinan Müftü Northeastern University	**Answer** I think it's a design problem. Someone needs to look at the parameters and the design. We have a web and wrap it around a cylinder then due to shell stiffness, it becomes more difficult to deform. But when we wrap it helically, the effective stiffness is reduced. The effective radius goes down. Moreover, you develop a stiffness not only in the longitudinal direction but also in the cross direction. That also plays into the problem.
Name & Affiliation David Pfeiffer JDP Innovations	**Question** I think in some printing press applications they use porous metal rolls to float the web. I think that allows them to float with a lesser flying height above the roll. Do you have any comment on that use rather than using holes?
Name & Affiliation Sinan Müftü Northeastern University	**Answer** I think in the old days the tape industry did the same thing. Instead of using rollers they wanted to minimize the friction drag on the motors so they were using porous guides essentially. In that case the clearance is much lower and the flow is not inertia dominated or it's somewhere in between on the lubrication side where there are some inertia effects. So you can get away with some corrections to the Reynolds equation. There, Eshel & Elrod, who came up with that famous equation, had some corrections to their equation. Interestingly, currently, the tape industry is using porous guides and the tape industry has the same problem as the web industry. The lateral control is very important and in fact probably more important for them because they can't tolerate mis-

registered tracks. They have tracks that are only 25 microns wide and the track widths going down for increasing areal densities. So they cannot afford the lateral motion. One of the things they've found is roller imperfections feed into lateral motion. So some companies are using porous guides which can be analyzed with the equations that you mentioned.

Name & Affiliation

Question

Yes, I would also think that with the porous guide, you would not have so much reduced shell stiffness with the helical wrap if you fly it alone for height the shell stiffness should be higher.

Name & Affiliation

Sinan Müftü
Northeastern University

Answer

That is a shell issue and something we cannot avoid if we're flying. When you're contacting that may be a different situation.